Biochimica et Biophysica Acta, 1056 (1991) 1–18
Elsevier

BBABIO 43314

A guide to electron paramagnetic resonance spectroscopy of Photosystem II membranes

Anne-Frances Miller [1] and Gary W. Brudvig [2]

[1] *Department of Biochemistry, Brandeis University, Waltham, MA (U.S.A.)* and [2] *Department of Chemistry, Yale University, New Haven, CT (U.S.A.)*

(Received 19 June 1990)

Key words: EPR; Photosystem II

Contents

Abbreviations: A_0 and A_1, two early electron acceptors in Photosystem I; Chl, chlorophyll; DCBQ, 2,5-dichloro-*p*-benzoquinone, an artificial electron acceptor to Photosystem II; DCMU, 3-(3,4-dichlorophenyl)-1,1-dimethylurea, an inhibitor of electron transfer from Q_A to Q_B; F_A, F_B and F_X, iron-sulfur center electron acceptors in Photosystem I; NADP, nicotinamide adenine dinucleotide phosphate; NADPH, reduced nicotinamide adenine dinucleotide phosphate; P680, the primary electron donor in Photosystem II; P700, the primary electron donor in Photosystem I; Ph, pheophytin, an early electron acceptor in photosystem II; PPBQ, phenyl-*p*-benzoquinone, an artificial electron acceptor to Photosystem II; Q_A, the primary quinone electron acceptor in Photosystem II; Q_B, the secondary quinone electron acceptor in Photosystem II; Y_D, a tyrosine electron donor in Photosystem II that gives rise to EPR signal II_{slow} when oxidized; Y_Z, a tyrosine electron donor in Photosystem II that in turn oxidizes the Mn complex.

Correspondence: A.-F. Miller, Department of Biochemistry, Brandeis University, Waltham, MA 02254, U.S.A.

Summary

This guide is intended to aid in the detection and identification of paramagnetic species in Photosystem II membranes, by electron paramagnetic resonance spectroscopy. The spectral features and occurrence of each of the electron paramagnetic resonance signals from Photosystem II are discussed, in relation to the nature of the moiety giving rise to the signal and the role of that species in photosynthetic electron transport. Examples of most of the signals discussed are shown. The electron paramagnetic resonance signals produced by the cytochrome b_6f and Photosystem I complexes, as well as the signals from other common contaminants, are also reviewed. Furthermore, references to seminal experiments on bacterial reaction centers are included. By reviewing both the spectroscopic and biochemical bases for the electron paramagnetic resonance signals of the cofactors that mediate photosynthetic electron transport, this paper provides an introduction to the use and interpretation of electron paramagnetic resonance spectroscopy in the study of Photosystem II.

I. Introduction

Electron paramagnetic resonance (EPR) spectroscopy monitors unpaired electrons directly. Thus, it is singularly appropriate for the study of electron transport, permitting one to observe paramagnetic electron carriers separately from the rest of the (diamagnetic) protein complex. EPR spectroscopy is also extremely sensitive, permitting the study of species present in micromolar or lower concentrations. A good introduction to EPR spectroscopy can be found in Knowles et al. [1], and Wertz and Bolton [2] have written a more complete treatise. In addition, Hoff [3] has written a clear and succinct discussion of EPR and related spectroscopies, and a brief summary of many of the EPR signals that are observed in photosynthetic systems. The current review presents a detailed discussion of the EPR

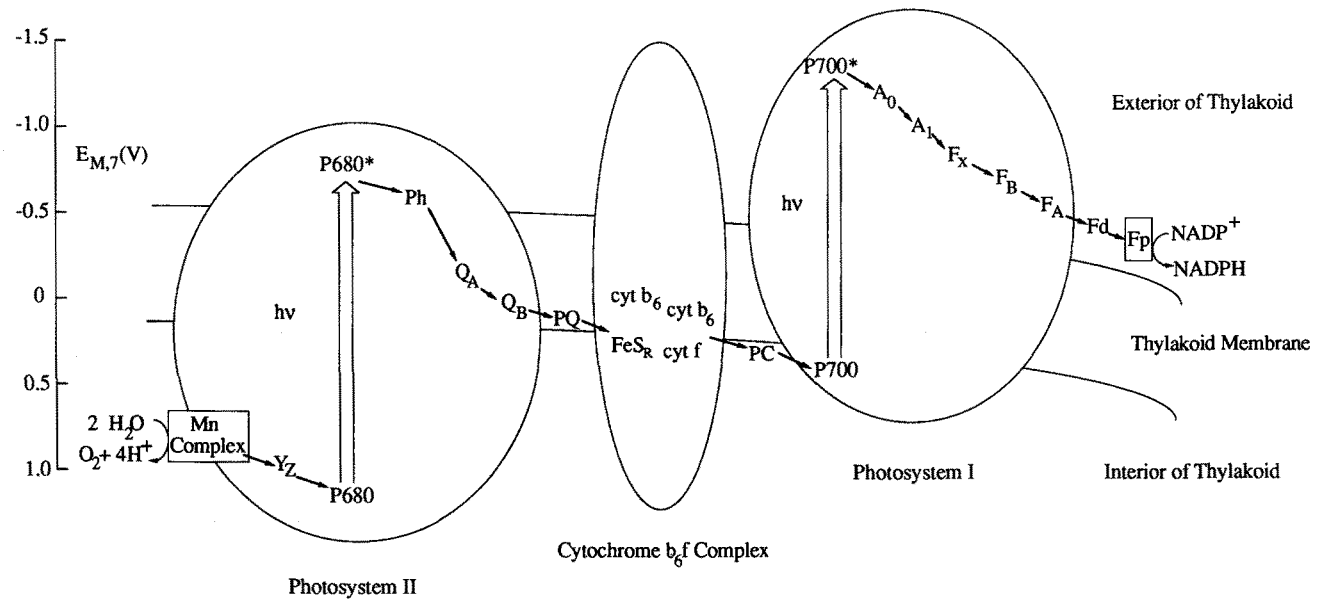

Scheme I. The Z scheme of photosynthetic electron transport in plants and cyanobacteria. The vertical position of each electron carrier corresponds to its reduction potential at pH 7. The double arrows signify photoexcitation and the solid arrows show the path of electron transport from water to $NADP^+$. Mobile electron carriers are shown outside the ovals that depict the membrane-bound protein complexes. Abbreviations in this scheme: cyt, cytochrome; Fd, ferredoxin; FeS_R, 'Rieske' iron sulfur center; Fp, flavoprotein ferredoxin nicotinamide adenine dinucleotide phosphate oxidoreductase; PC, plastocyanin; PQ, plastoquinone. Adapted from Ref. 147.

signals originating from Photosystem II, as well as other components of the photosynthetic membranes of higher plants, and relates the information these signals provide to the nature of the species from which the signals arise and the roles of the species in photosynthetic electron transport.

Photosystem II is the first in the series of three complexes that couple photochemical excitation of electrons to electron transport from H_2O to $NADP^+$ in higher plants (Scheme I, reviewed in Refs 4–6 and others in that volume). Photosystem II, the cytochrome b_6f complex and Photosystem I are complicated assemblies of protein and cofactors, embedded in the thylakoid membranes of chloroplasts. Photosystem I mediates light-driven production of oxidized plastocyanin and the strong reductant NADPH, from reduced plastocyanin and $NADP^+$. Reduction of plastocyanin by plastoquinol is coupled to transmembrane H^+ transport by the cytochrome b_6f complex. But first of all, Photosystem II uses photochemical energy to produce plastoquinol and O_2 from plastoquinone and H_2O. Each of these segments of the photosynthetic electron transport chain involves the participation of a number of redox cofactors, in addition to the two mobile electron carriers that connect them, plastocyanin and plastoquinone. The sequence of carriers by which electrons

TABLE I

Key to EPR signals that may arise in Photosystem II membranes

Signals arising from Photosystem II are described in boldface type and signals arising from Photosystem I, the cytochrome b_6f complex, contaminating metal ions and O_2 are described in plain type.

g value	Width	Observation temperature and microwave power [a]	Identity	Section in text, and figure numbers in parentheses [b]
5–8	**≈ 5 mT ea**	**4–5 K, 20–50 mW**	**Q_{400}, = $Fe^{3+}Q_A$**	**II-L (7, 8)**
6	≈ 5 mT	8–15 K, 0.2–20 mW	assorted high-spin cytochromes	III-A (3, 8, 9)
4.2	20 mT	4–25 K, 0.2 mW and up	rhombic Fe^{3+}	IV-A (3, 8, 9)
4.1	**20 mT**	**4–15 K, 0.2 mW**	**S_2-state of Mn complex**	**II-D (3)**
Throughout range	variable	4–25 K, 0.2 mW and up	O_2	IV-D (9)
3.5 to 3.6	≈ 4 mT	8–15 K, 0.2–20 mW	cytochromes b_6 and f	III-A (8)
3.1–2.9 = g_z	**4 mT**	**10–15 K, 4 mW**	**cytochrome *b*-559**	**II-E (4, 8, 9)**
2.2–2.1 = g_y				
2.05 = $g_\perp$	60 mT	4–300 K, saturates easily		
2.24 = $g_\parallel$		at lower (1 He) temperatures	Cu^{2+}	IV-B (4, 9)
2.0	100 mT a = 9.5 mT	4–300 K, 0.2 mW and up	$Mn^{2+}(H_2O)_6$	IV-C (8)
1.96	**200 mT** **≥ 16 lines** **a = 5.0–9.0 mT**	**7 K, 0.2 mW**	**S_2-state of the Mn complex 'multiline signal'**	**II-C (3, 7, 9)**
2.0046	**1.9 mT**	**10 K to room temp. 10 μW to 0.2 mW**	**Tyr radicals Y_D^+ and Y_Z^+**	**II-A, II-I (1, 8)**
2.0035	**1.25 mT**	**80 K, 0.1 mW**	**Ph^-**	**II-H**
2.0	**split by 3–5 mT**	**4–5 K, 20 mW**	**$Fe^{2+}Q_A^-Ph^-$**	**II-G (5)**
2.0026	**1.0–1.1 mT**	**100 K to room temp. 0.1 mW**	**Chl cation radical**	**II-F (1)**
	≈ 0.8 mT	**100 K to room temp. 0.1 mW**	**$P680^+$**	**II-J**
	≈ 0.7 mT	100 K to room temp. 0.1 mW	$P700^+$	III-C
2	**extends over 60 mT**	**3–5 K, 10 μW**	**$^3P680$**	**II-K (6)**
2	extends over 60 mT	3–11 K, 10 μW	$^3P700$	III-C
2.0–1.8	2.0 mT	7–20 K, 0.2–2 mW	Rieske iron-sulfur center	III-B (3, 4)
2.05–1.75	2.0 mT	10–25 K, 1–20 mW	Fe_4S_4 centers F_A, F_B and F_X	III-E
1.82 & 1.67 and 1.90 & 1.64	**30 mT** **40 mT**	**4–10 K, 4–50 mW**	**$Fe^{2+}Q_A^-$**	**II-B (2, 3, 7)**

[a] This table only lists observation temperatures above 4 K, although many signals may be observable at lower temperatures [150]. Furthermore, the temperatures and powers are representative only, intended to serve as convenient starting-points for those wishing to observe a signal for the first time. The optimum temperature and power will depend considerably on the instruments being used and the experimental context. Indeed, temperatures and powers outside the ranges listed (especially lower temperatures and powers) are often used. However, when observing free radicals at liquid He temperatures, it may be difficult to avoid microwave power saturation.

[b] Often several figures in which a signal can be recognized are listed. However, the numbers of figures in which a signal features prominently are underlined, for emphasis.

are believed to pass from H_2O to $NADP^+$ is shown in Scheme I. EPR signals have been identified from all of the carriers shown.

Photosystem II alone comprises a daunting array of different electron carriers, with diverse EPR signals. However, our understanding of electron transport in Photosystem II has benefitted a great deal from earlier work on the photosynthetic reaction centers of purple non-sulfur bacteria (reviewed in Refs. 7, 8). The bacterial reaction centers do not draw electrons from H_2O. Therefore, they operate at different reduction potentials and employ different electron donation pathways from photosystem II. However, the electron acceptance pathways of the bacterial reaction centers and Photosystem II have long been recognized to be analogous (for comparisons see Refs. 7, 9). In both cases, electrons are transferred from the primary electron donor to a pheophytin, on to a quinone that accepts one electron, and then to a quinone that accepts two electrons. Furthermore, the kinetics are similar, at each of the steps, and the analogous electron carriers produce almost identical EPR signals in bacterial reaction centers and Photosystem II. These biophysical similarities go hand in hand with striking biochemical parallels, in the protein compositions of the core complexes [10], and their amino acid sequences [11]. Thus, the importance of the bacterial reaction center as a model for Photosystem II extends well beyond the X-ray crystal structure of the bacterial reaction center, and discussions of EPR signals that are observed in bacterial reaction centers as well as Photosystem II include references to both literatures.

In addition, although Photosystem II is not usually studied in its natural context of chloroplast membranes, the more commonly used Photosystem II-enriched preparations occasionally contain significant residual amounts of the cytochrome b_6f complex and Photosystem I. Therefore, EPR signals from these two complexes are also mentioned briefly. Thus, it is hoped that this review will provide an introduction to EPR spectroscopy of Photosystem II of wide interest and utility.

For each of the EPR signals from Photosystem II, the conditions for generating the signal are described, and related to the biochemical activity of the species from which it arises. In addition, the identifying spectral characteristics are listed and related to the nature and environment of each paramagnetic species. All spectra shown were collected at X-band (9.1 GHz) and, unless otherwise stated, all samples were prepared as in Refs. 12 and 13 and suspended in buffers containing 30% (v/v) ethylene glycol as a cryoprotectant. Finally, an identification key based on approximate g values, signal widths and conditions of observation is provided for rapid preliminary identification of unfamiliar signals (Table I). The key refers the reader to figures and descriptions in the text for more definitive signal assignments.

II. Electron transport components of Photosystem II

Ultimately, EPR experiments depend on the possibility of generating the paramagnetic states of species for observation, that is to say species with unpaired electron(s). Although many biochemicals do not usually have unpaired electrons, transport of single electrons is the normal activity of most of the cofactors of Photosystem II. In general, only alternate oxidation states of a given species are paramagnetic and have an EPR signal. As a result, most of the photosynthetic electron carriers give rise to a signal either in the dark-adapted state or after a flash of light (and charge separation), but not both. The paramagnetic states of most species in Photosystem II are generated upon illumination.

Scheme II shows the components of Photosystem II, their approximate reduction midpoint potentials and the paths of electron transport among them (reviewed in Refs. 6, 14). This scheme illustrates how one can produce a paramagnetic oxidation state of a given component of Photosystem II by manipulating the electrochemical potential of the medium, or by driving electron transport through a selected portion of the electron transport chain. The latter is conveniently achieved with light, by illuminating in the presence of inhibitors of certain electron transport steps, after specific inhibitory treatments, or at temperatures chosen to favor a particular pathway of electron transport. Numerous ingenious combinations of these strategies have enabled researchers to generate a paramagnetic state of each species in the photosynthetic electron transport chain, even if only transiently.

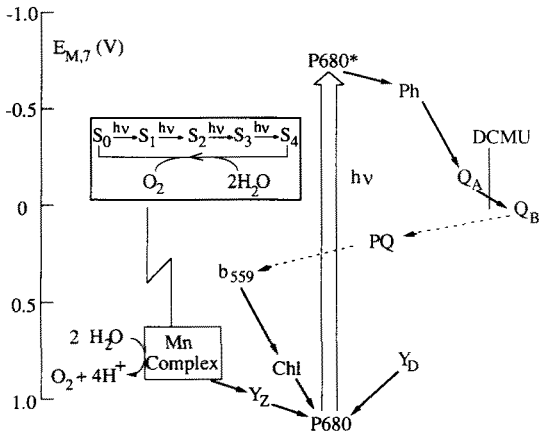

Scheme II. Electron transport among components of Photosystem II. The components of photosystem II are shown with a vertical placement corresponding to their reduction potential. The path of electron acceptance and the three competing paths of electron donation are shown in detail, along with the site of inhibition by DCMU. Inset: the Mn complex is believed to cycle through five oxidation states in the course of accumulating oxidizing equivalents from P680 and then applying them to two water molecules and releasing molecular oxygen. Abbreviations in this scheme: PQ, plastoquinone; b_{559}, cytochrome b-559.

A short saturating flash of light will cause a single charge separation in every Photosystem II center at 273 K. An unpaired electron is rapidly transferred from the primary electron donor (P680) to pheophytin (Ph), then to Q_A, and on to Q_B (Scheme II). The resulting $P680^+$ is rereduced by a series of electron donors (Scheme II). Thus, the photoexcited, highly reducing electron moves away from the primary electron donor, along the electron acceptance chain, and the oxidizing vacancy left in $P680^+$ also is effectively transferred away, to reside on an electron donor, instead of recombining with the photoexcited electron. Thus, a reduced electron acceptor and an oxidized electron donor are the products of each stabilized charge separation. These can be trapped by rapidly cooling an illuminated sample to 77 K, provided the sample does not contain compounds capable of reacting with either charged species.

Although many paramagnetic species in Photosystem II can be produced during illumination and trapped by cooling to 77 K immediately, for observation later, others decay away during the time necessary to cool a sample, and may not be stabilized at 77 K. However, during intense continuous illumination, a relatively large steady-state population of some of these short-lived species can be produced. Extremely short-lived species can only be observed transiently with time-resolved detection methods. The paramagnetic species that can be generated in Photosystem II will be discussed beginning with the most stable and simple to observe, and progressing to shorter-lived species and signals which are observed only under special conditions.

II-A. Tyrosine Y_D^+ radical

Only one component of Photosystem II is normally visible by EPR in Photosystem II membranes that have been allowed to dark-adapt (at 273 K): the tyrosine radical Y_D^+. Y_D is a tyrosine residue that can donate an electron to $P680^+$ [15], but does not appear to participate directly in O_2 evolution [16,17]. The photooxidized state, Y_D^+, produces an EPR signal, but in Photosystem II membranes, only roughly 25% of the Y_D^+ formed during continuous illumination is rereduced to Y_D in darkness. Therefore, the signal from Y_D^+ can persist in up to 75% of Photosystem II centers that have been extensively dark adapted (Fig. 1a). (The 25% has been proposed to represent Photosystem II centers that contain the S_0 state of the Mn complex when illumination ceases, and the loss of Y_D^+ is explained by electron transfer between Y_D^+ and the Mn complex: $S_0Y_D^+ \rightarrow S_1Y_D$, $\tau_{1/2} \approx$ tens of minutes [18,19].) A larger fraction of Y_D^+ is rereduced during dark-adaptation of thylakoid membranes, but nonetheless, significant amounts persist [20].

The EPR signal of Y_D^+ has a g value of $g = 2.0046$, a linewidth of 1.9 mT, and partially-resolved hyperfine

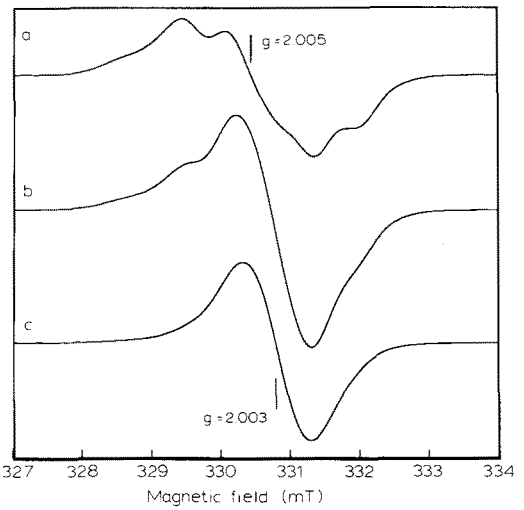

Fig. 1. The effect of illumination on free radical signals in Photosystem II membranes. (a) collected from dark-adapted Photosystem II membranes in the dark, shows a signal from Y_D^+ only ($g = 2.0046$). (b) collected from the same sample after illumination at 77 K for 10 min (with cytochrome *b*-559 chemically oxidized), contains the signal of photooxidized Chl as well as Y_D^+. Upon subtraction of the dark spectrum (a) from the post-illumination spectrum (b), the difference spectrum (c) shows the photoinduced Chl^+ signal ($g = 2.0026$). Instrument conditions: sample temperature, 100 K; microwave power, 0.2 mW; microwave frequency, 9.1 GHz; magnetic field modulation frequency, 100 kHz; magnetic field modulation amplitude, 0.4 mT.

peaks approx. 0.5 mT apart [21,22] (first reported by Commoner et al. [23]). (Although the Y_D^+ notation is used to specify the photooxidized state of Y_D, this species is not necessarily cationic [24].) Y_D was identified as a tyrosine residue by Barry and Babcock [25], specifically Tyr 160 of the D2 polypeptide of Photosystem II in *Synechocystis* [16,17]. Thus, the 1:3:3:1 intensity ratio of the features of the signal from Y_D^+ can be explained by hyperfine coupling of the unpaired electron to two ring protons and one methylene proton. This methylene proton is proposed to have the same hyperfine coupling constant as the ring protons, due to the size of the dihedral angle between its bond to the methylene carbon and the ring plane [25].

There are, in fact, several EPR signals with the same lineshape, all called signal II, that can be distinguished by their kinetics. The one due to Y_D^+ is called signal II_{slow} (signal II_s) because it decays slowly in the dark. So-called signals II_f and II_{vf} (fast and very fast), which arise from Y_Z^+ instead of Y_D^+, decay on millisecond and microsecond time scales, and cannot easily be detected except during continuous illumination (see subsection II-I). Recently, a signal II has been produced in CP47/D1/D2/cytochrome *b*-559 preparations [26].

Y_D^+ can be generated at every Photosystem II center by illumination at 273 K for a minute or so, and trapped by cooling to 77 K. The resulting EPR signal can easily be observed over a wide range of temperatures (< 10 K to room temperature); however, it

saturates easily at lower temperatures [27]. The area of the signal from Y_D^+ (obtained by integrating twice) can be used as a standard for one spin per Photosystem II center [28] in quantitations of other free radical signals, such as that of Chl^+ [29]. Note, however, that Y_D^+ is reduced slowly by cytochrome *b*-559 at 200 K ($\tau_{1/2} \approx$ weeks, [30]), and recombines with Q_A^- slowly, even at 77 K ($\tau_{1/2} \approx$ days, [31,32]), so spectra to be used for quantitations should be collected relatively soon after illumination.

During O_2 evolution, electron donation from Y_D (and from cytochrome *b*-559 via Chl) is much slower than electron donation by Y_Z, the Mn complex, and ultimately, H_2O (see Scheme II). Therefore, the latter path dominates and, in O_2-evolving Photosystem II membranes that have previously been dark-adapted, the products of charge separation at room temperature are the S_2-state of the Mn complex, and reduced Q_A. The EPR signals of these two species will be discussed in turn.

II-B. The semiquinone-iron complex: $Fe^{2+}Q_A^-$

Quinone A (Q_A) is an electron acceptor in Photosystem II. It normally accepts a single electron, and is the first carrier in the electron acceptance chain at which the unpaired electron resulting from charge separation is stable on the time-scale of milliseconds. By the time the electron reaches Q_A, dissipation of a large fraction of the photoexcitation energy (see Scheme II), and physical separation of the reduced product from the oxidized product of charge separation decrease the likelihood of recombination between the two.

Photoreduced Q_A is a semiquinone anion radical, and interacts with a nearby Fe^{2+} ion (see Ref. 33), to produce a 40 mT wide (trough to trough) signal at $g = 1.90$ and 1.64, or a narrower signal at $g = 1.82$ and 1.67 (Fig. 2, first observation of $Fe^{2+}Q_A^-$ in Photosystem II [34]). These two signals represent alternate forms of the $Fe^{2+}Q_A^-$ pair, and are best observed at liquid He temperatures (4 K) and high powers of microwave irradiation (20 mW). At higher pH, the $g = 1.90$ form of $Fe^{2+}Q_A^-$ predominates, whereas at lower pH the $g = 1.82$ form is observed [35]. Displacement of essential CO_2/HCO_3^- from Photosystem II by formate greatly increases the amplitude of the $g = 1.82$ signal from $Fe^{2+}Q_A^-$ [36]. In addition, some herbicides alter the width of the $Fe^{2+}Q_A^-$ $g = 1.82$ signal, possibly because of their mode of binding in the Q_B-binding site [37]. Bacterial photosystems most often display the $g = 1.82$ $Fe^{2+}Q_A^-$ signal [38], but bacterial $g = 1.9$ signals have also been observed [8]. (The shape and magnetic properties of the bacterial signal have been investigated in detail and explained in terms of two doublets resulting from antiferromagnetic coupling of the semiquinone radical with the Fe^{2+} ion [39]; however, see the discussion in Ref. 40.)

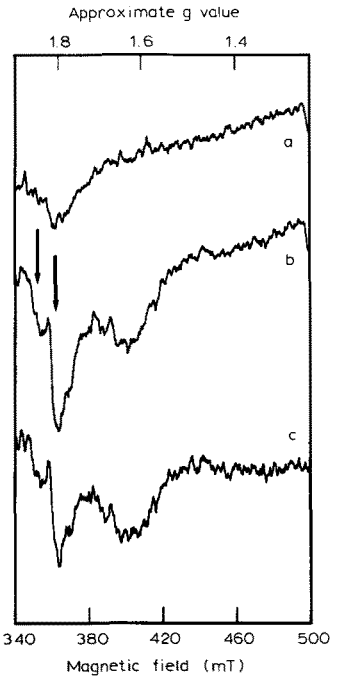

Fig. 2. The effect of illumination on the primary quinone electron acceptor of Photosystem II. (a) The background (dark) spectrum collected prior to illumination. (b) The spectrum collected under the same conditions after illumination at 77 K for 10 min. (c) The (illuminated-dark) difference spectrum shows the EPR signals arising from both types of $Fe^{2+}Q_A^-$ complex ($g = 1.82$ and 1.67, and $g = 1.90$ and 1.64). The arrows indicate the $g = 1.9$ and $g = 1.82$ turning points. Instrumental conditions: sample temperature, 4 K; microwave power, 22 mW; microwave frequency, 9.1 GHz; magnetic field modulation frequency, 100 kHz; magnetic field modulation amplitude, 2.0 mT.

After removal of the iron ion; Photosystem II membranes display a signal from the plastosemiquinone radical Q_A^- alone, at $g = 2.0044 \pm 0.0003$ with a linewidth of $\Delta H = 0.9$ mT [41]. This signal is also observed upon removal of iron from bacterial reaction centers, and is replaced by the usual signal after reconstitution of iron [42]. The EPR signal from $Fe^{2+}Q_B^-$ has also been observed in bacterial reaction center preparations [43,44]. Similarly, when Photosystem II is illuminated at low temperature to produce $Fe^{2+}Q_A^-$, and then annealed at temperatures near 273 K, to permit electron transfer to Q_B, a signal slightly different from that of $Fe^{2+}Q_A^-$ is observed. This signal has been ascribed to $Fe^{2+}Q_B^-$ [45] (also see Ref. 46).

If illumination is performed at temperatures below 230 K, electron transport from Q_A to Q_B and beyond is extremely slow, and the negative charge resulting from charge separation can be trapped on Q_A by rapid cooling (to prevent recombination). Alternately, or in addition, 100 μM DCMU can be used to inhibit electron transport beyond Q_A with the same results (as in Ref. 13). Truncation of the electron-acceptance chain at Q_A restricts Photosystem II to stabilizing a single charge

separation under normal conditions, because Q_A can only accept one electron (and reduced pheophytin back-reacts readily with oxidized electron donors, Scheme II). Furthermore, extended illumination (1–2 min) of Photosystem II with the electron transport chain truncated at Q_A results in production of Q_A^- in every Photosystem II center that stabilizes a charge separation. Therefore, the magnitude of the $Fe^{2+}Q_A^-$ EPR signal resulting from illumination, in the presence of DCMU, serves as an indicator of the fraction of Photosystem II centers that have stabilized a charge separation [29]. Note, however, that the control sample should also contain DCMU, because in addition to enhancing the yield of $Fe^{2+}Q_A^-$, this inhibitor may also affect the $Fe^{2+}Q_A^-$ signal intensity [37].

II-C. The S_2 state of the Mn complex: the multiline signal

Photosystem II mediates a four-electron reaction ($2H_2O \rightarrow O_2$) as it cycles through five oxidation states called S states (Scheme II, inset). The S_1 state has accumulated one oxidizing equivalent, S_2, two, and so on. In the course of normal activity, each photon absorbed by P680 leads to an advance in the S state up to S_4, which returns to S_0 upon release of O_2 in a light-independent reaction [47].

The dark-stable state is S_1, and after a single saturating flash of light, the S_2 state is generated. An EPR signal originating from a Mn complex is also produced after a single saturating flash of light. Furthermore, the amplitude of this 'multiline' signal oscillates with the number of illuminating flashes, with a period of 4 [48]. This behavior identifies the multiline signal with the S_2 state, and is consistent with accumulation of oxidation equivalents for O_2 evolution by the Mn complex from which the signal arises. The fact that the S_2-state of the Mn complex displays EPR signals suggests that the S_0 and S_4 states might also. Unfortunately, no signals from either of these states have been observed yet.

The S_2 state of the Mn complex is stable for a minute or so at 273 K, and can be trapped for observation by cooling a sample of Photosystem II membranes to 77 K immediately after a flash of light, or after illumination in the presence of DCMU. In thylakoid membranes, or in the presence of added electron acceptors that prevent Q_A^- from recombining with it, the S_2 state is even longer-lived ($\tau_{1/2} \approx 5$ min at 273 K [49,50]). The S_2-state multiline EPR signal is observed conveniently at approx. 7 K (Figs. 3, 7 and 9). The g value and overall width of the signal, as well as the number of hyperfine lines are indicative of a mixed-valence cluster of exchange-coupled Mn ions [48]. The signal appears to be fairly isotropic with respect to g value when observed at 9 GHz ($S = \frac{1}{2}$, $g = 1.98$ [51]), and is dominated by hyperfine coupling to at least two ^{55}Mn nuclei ($a = 7.5$–9.0 mT [48]). EPR spectra observed at 3.9 GHz (S band)

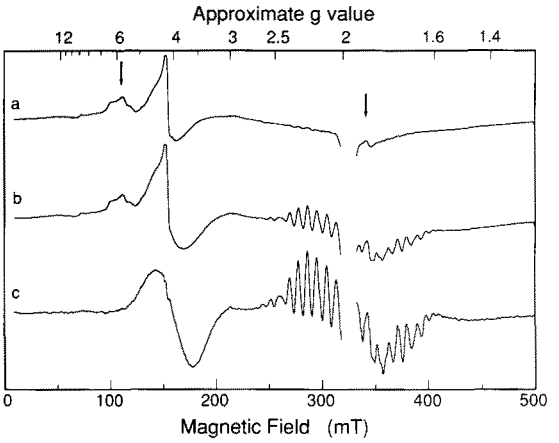

Fig. 3. Formation of the S_2 state $g = 4.1$ and multiline signals: The effect of illumination at 200 K in buffer containing 0.4 M sucrose as the cryoprotectant. (a) A spectrum collected from dark-adapted Photosystem II membranes in the dark, showing the signal rom rhombic iron at $g \approx 4.2$. Arrows indicate signals from high-spin cytochromes ($g_\perp \approx 6$) and Rieske Fe_2S_2 ($g \approx 1.9$). (b) Spectrum after illumination at 200 K for 2 min, showing an increase in EPR intensity at $g \approx 4$ as well as the S_2-state multiline signal at $g \approx 2$. The difference spectrum (c) clearly shows the S_2-state $g = 4.1$ signal and the multiline signal (with contributions from the underlying $Fe^{2+}Q_A^-$ signals). Spectrum (c) is shown magnified by a factor of three relative to spectra (a) and (b). Similar results are obtained by illuminating samples containing 30% ethylene glycol at temperatures between 130 K and 160 K. Instrument conditions: sample temperature, 7 K; microwave power, 0.2 mW; microwave frequency, 9.1 GHz; magnetic field modulation frequency, 100 kHz; magnetic field modulation amplitude, 2.0 mT.

have provided evidence for hyperfine anisotropy in the S_2-state multiline signal [52] (also see Ref. 40).

Because the spectral characteristics of the multiline signal reflect the strength with which the Mn ions of the Mn complex are coupled with one another, the multiline signal has been a valuable indicator of changes in the structure of the Mn complex. The S_2-state multiline signal from Photosystem II membranes treated with $H_2{}^{17}O$ shows slight line broadening due to coupling with ^{17}O ($I = \frac{5}{2}$), and thus, evidence of coordination to Mn of O derived from H_2O [53]. Upon treatment of Photosystem II with the substrate analog NH_3, the S_2-state multiline signal is altered ($a = 7$ mT [54,55]), suggesting a direct interaction between NH_3 and the Mn complex. This has been confirmed by electron spin echo envelope modulation spectroscopy [56]. Thus, EPR spectroscopic evidence has been used to argue that the Mn complex is both the site of substrate binding and oxidation.

Ca^{2+}-depleted (extrinsic polypeptide-complete) Photosystem II membranes exhibit another type of multiline signal ($a = 5.5$ mT) [57–59], and the (S_2) state from which the signal originates is stable for hours in darkness at 273 K. In addition, substitution of Sr^{2+} for Ca^{2+} also results in an S_2-state multiline signal with smaller than normal hyperfine splitting ($a = 7$ mT) [60]. These results, and those discussed in subsection II-M,

demonstrate that Ca^{2+} exerts an important direct or structural influence on the Mn complex and electron donation in Photosystem II. Proposed structures for the Mn complex, mechanisms of O_2 evolution and a possible role for Ca^{2+} are reviewed in Refs. 61,62 (see also Ref. 59).

II-D. The S_2 state of the Mn complex: the $g = 4.1$ signal

A common way of trapping transient intermediates is to perform a reaction at temperatures at which initial intermediates are formed but later step(s) are inhibited. The primary photochemistry of photosynthesis proceeds even at the lowest temperatures obtainable, by a temperature-independent tunnelling mechanism [63]. Thus, there is no lower limit to the temperatures that can be used to generate intermediates, but for the same reason, it is impossible to trap primary charge-separated states. Nonetheless, important insights into the different competing pathways of electron donation in Photosystem II have been obtained by comparing the products of illuminations conducted at a range of temperatures.

Illumination at 160 K and above in the presence of DCMU produces constant amounts of multiline signal, accounting for approximately one oxidizing equivalent per Photosystem II center [29]. However, below 160 K the amplitude of the S_2-state multiline EPR signal varies with the temperature of illumination as a result of temperature-dependent Mn complex conformation changes (160–120 K) and a temperature-dependent rate of oxidation to the S_2-state (130–77 K) [29].

Illumination between 160 K and 120 K results in decreasing yields of S_2-state multiline EPR signal with decreasing illumination temperature, and compensating increases in production of the S_2-state $g = 4.1$ EPR signal (Fig. 3c) [29], although the choice of cryoprotectant affects the exact amount of $g = 4.1$ signal formed at a given illumination temperature [64]. In Cl^--sufficient media the $g = 4.1$ signal is replaced by the S_2-state multiline signal upon annealing at 200 K in darkness [29,65], and the amplitude of the $g = 4.1$ signal displays the same oscillation with number of flashes of light as does the S_2-state multiline signal [64]. Therefore, the $g = 4.1$ signal has been assigned to Mn, in the S_2 state, in a configuration trapped by illumination at low temperatures [29,64], and favored by Cl^- depletion [66] or substitution with F^-, CH_3NH_2 or NH_3 [65,67]. The effects of Cl^- on the spectroscopic form of the Mn site suggest a connection between Cl^- (which is essential for catalytic activity) and the conformation or electron-donation properties of Mn in Photosystem II (discussed in Ref. 68). However, no superhyperfine coupling to Cl^- is observed in studies of the multiline signal [52,69].

The S_2-state $g = 4.1$ signal is named after its g value of 4.1 and is approx. 34 mT wide (peak to trough) [70,65]. It is apparent only as a broadening of the $g = 4.2$ rhombic iron signal upon illumination, in spectra collected at temperatures of about 7 K. However, when a spectrum collected before illumination is subtracted from the spectrum collected afterwards, the difference spectrum of a sample illuminated at 130 K to 170 K displays a prominent $g = 4.1$ signal (Fig. 3). The g value of approx. 4 is suggestive of an $S = \frac{3}{2}$ state, and is consistent with either an isolated Mn^{IV} ion or a tetranuclear structure (Refs. 51 and 71, respectively).

II-E. Cytochrome b-559

Each Photosystem II center contains two *b*-type cytochromes, characterized by an absorption maximum near 559 nm, and therefore called cytochromes *b*-559. These have been proposed to mediate protective cyclic electron transport in Photosystem II [72] (Scheme II). Below 130 K, the total extent of Mn complex photooxidation decreases with decreasing temperature of illumination, and increasing amounts of photooxidized cytochrome *b*-559 are observed instead, as the branching ratio between the two competing pathways changes (Scheme II). At 77 K, cytochrome *b*-559 is photooxidized exclusively, in amounts corresponding to one heme per Photosystem II center [29].

Oxidized cytochrome *b*-559 has a low-spin Fe^{3+} heme ($S = \frac{1}{2}$). The rhombic symmetry about the Fe^{3+} results in g anisotropy, and the turning points at $g_z \approx 3$ and $g_y \approx 2.2$ are easily observed in spectra collected at about 10 K (Fig. 4). The g_x turning-point, however, is very broad, and is not prominent in Photosystem II membranes ($g_x \approx 1.5$ for isolated cytochrome *b*-559 [73]). Detailed studies of the g values and the Raman spectrum of cytochrome *b*-559 have been interpreted to indicate that the heme is ligated by histidines, from the 4.5 and 10 kDa polypeptides of Photosystem II [73]. Finally, the orientation dependence of the EPR spectrum of cytochrome *b*-559 indicates that the heme plane is perpendicular to the thylakoid membrane [74].

Cytochrome *b*-559 is believed to occur in two or three different forms characterized by different reduction midpoint potentials, and called low-, intermediate- and high-potential cytochrome *b*-559, as appropriate [75,76]. Low-potential cytochrome *b*-559 has a reduction potential of ≈ 0 mV, and therefore is normally oxidized and visible in EPR spectra of dark-adapted Photosystem II membranes. Depletion of the 17 and 23 kDa extrinsic polypeptides results in loss of high-potential cytochrome *b*-559 and appearance of low-potential cytochrome *b*-559 instead [75,77]. Therefore, the presence of oxidized cytochrome *b*-559 in samples that have been rigorously maintained in darkness is sometimes indicative of polypeptide loss (Fig. 8). Nevertheless, low-potential cytochrome *b*-559 is not necessarily photochemically inactive, as cytochrome *b*-559 can be photooxidized in all Photosystem II centers, even when

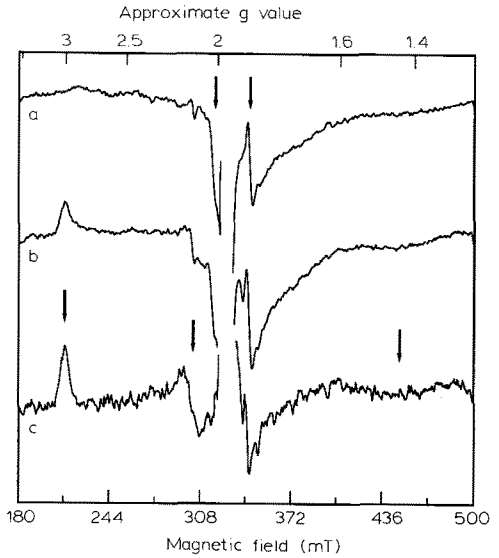

Fig. 4. Photooxidation of cytochrome *b*-559. (a) A spectrum of dark-adapted untreated Photosystem II membranes shows only small amounts of oxidized cytochrome *b*-559 at $g \approx 2.9$. The dark scan also shows the usual signal from Cu^{2+} at $g_{\perp} = 2.05$ and Rieske Fe_2S_2 at $g_y = 1.90$ (indicated by arrows). Upon illumination at 77 K for 10 min, cytochrome *b*-559 is photooxidized and Q_A is reduced. (b) Cytochrome *b*-559 is prominent in the spectrum collected after illumination, at $g_z = 3.08$ and $g_y = 2.15$, and possibly $g \approx 1.43$. The $Fe^{2+}Q_A^-$ signal is not prominent, because the spectra were collected at a higher temperature and lower microwave power than are optimal for observation of $Fe^{2+}Q_A^-$, in order not to saturate the cytochrome *b*-559 signal. (c) The (illuminated-dark) difference spectrum, magnified 2-fold, shows high-potential photooxidized cytochrome *b*-559 trapped at 77 K, with the turning points indicated by arrows. O_2 cannot be ruled out as the source of the turning point at $g \approx 1.43$ (see Fig. 9). Instrument conditions: sample temperature, 10 K; all other parameters as in Fig. 3.

these lack the extrinsic polypeptides, so long as the cytochrome is (chemically) reduced prior to illumination [75,78,79].

Cytochrome *b*-559 displays slightly different *g* values in untreated and polypeptide-depleted Photosystem II membranes. In addition, the *g* values observed upon photooxidation at 77 K, and after annealing at 273 K or chemical oxidation at 273 K differ from one another [75]. The *g* values observed after illumination at 77 K have been interpreted to reflect trapping of cytochrome *b*-559 in the conformation typical of its reduced state, in contrast to the *g* values observed after equilibration at 273 K, which reflect the preferred conformation of oxidized cytochrome *b*-559. The *g*-value shifts upon polypeptide depletion have been suggested to indicate a conformationally-induced change in the solvent accessibility of cytochrome *b*-559 [75].

II-F. Chlorophyll

Cytochrome *b*-559 is photooxidized via chlorophyll in Photosystem II [72] (Scheme II). However, when cytochrome *b*-559 is (chemically) oxidized prior to illumination, and thus unable to rereduce Chl^+, Chl^+ can be trapped for observation after illumination at 230 K or below [80,81]. Chl^+ is a relatively unstable free radical (with a half-life on the order of hours at 77 K). The EPR signal from Chl^+ is evident when superimposed on that of Y_D^+ as an increase in signal intensity at the highest-field maximum of the signal from Y_D^+ (Fig. 1b). Subtraction of the signal due to Y_D^+ reveals the simple gaussian signal of Chl^+ at $g = 2.0026$ [80] with a linewidth of 1.0–1.1 mT (Fig. 1c).

At illumination temperatures above 230 K, the short lifetime of Chl^+ results in only a small steady-state population [82]. In contrast, at 77 K, illumination of polypeptide-complete samples with chemically oxidized cytochrome *b*-559 results in photooxidation of one chlorophyll per Photosystem II center [29]. In samples lacking extrinsic polypeptides, however, only a fraction of the Photosystem II centers stabilize $Chl^+Fe^{2+}Q_A^-$ [83]. Thompson and Brudvig [72] have proposed that the Chl^+ EPR signal emanates from a specific Chl moiety that acts to transfer energy to the primary electron donor, and is particularly susceptible to photooxidation and damage as a consequence of its necessary proximity to P680. A signal similar to that of Chl^+ has been observed in D1/D2/cytochrome *b*-559 preparations, supporting its assignment to a Chl closely associated with the reaction center [84].

II-G. Pheophytin: the split signal

Just as prior oxidation of cytochrome *b*-559 is necessary to permit trapping of Chl^+, conditions that maintain Q_A in its reduced state permit accumulation of the paramagnetic state of the electron acceptor that precedes it: pheophytin (Ph). In the course of illumination at 200 K in the presence of (50 mM) dithionite, oxidized electron donors can be rereduced, but reoxidation of photoreduced Ph is prevented and the Ph^--radical anion can be trapped for observation (Fig. 5, Ph is also called I, for *I*ntermediate electron acceptor). The signal of Ph^- in the presence of $Fe^{2+}Q_A^-$ is split by 3–5 mT, due to exchange coupling with $Fe^{2+}Q_A^-$ [41] ([85] for examples of the bacterial signal). The magnitude of the splitting depends on the form of the $Fe^{2+}Q_A^-$ complex (subsection II-B), with the $g = 1.82$ form giving a smaller splitting, and the $g = 1.9$ form giving a larger splitting [35]. The split pheophytin signal does not saturate as easily as the signal of Ph^- observed in the absence of $Fe^{2+}Q_A^-$, and can therefore be observed at lower temperatures or higher microwave powers than the simple Ph^- free radical signal, as a result of the Fe^{2+} character imparted to Ph^- by the interaction between it and $Fe^{2+}Q_A^-$ [41,86].

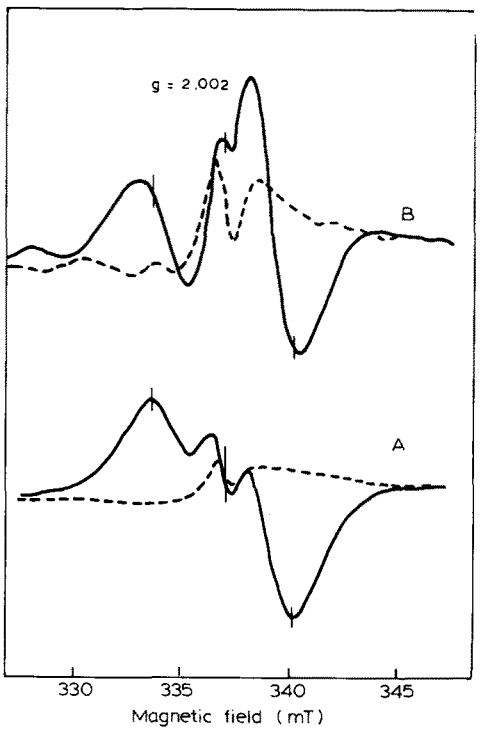

Fig. 5. The split signal from Ph^- interacting with $Fe^{2+}Q_A^-$. In each case, Ph^- was generated in the presence of $Fe^{2+}Q_A^-$ by illumination for 4 min at 200 K in the presence of 50 mM sodium dithionite. The spectra of the dithionite-treated Photosystem II membranes [35] prior to illumination (dotted lines) are shown as well as the post-illumination spectra (solid lines). The two different cases shown are Photosystem II membranes suspended in media of two different pH levels: (A) Bottom, pH 6; (B) top, pH 8.5. Thus, the top and bottom spectra represent Ph^- in the presence of the two different forms of the $Fe^{2+}Q_A^-$ complex: the $g = 1.90$ and $g = 1.82$ forms, respectively. Sucrose was used as the cryoprotectant, the three tickmarks identify equivalent magnetic field positions in the two illuminated spectra, and the center tickmark corresponds to $g = 2.002$ [35]. Instrument conditions: sample temperature, 4–5 K; microwave power, ≈ 35 mW; microwave frequency, 9.45 GHz; magnetic field modulation amplitude, 1.0 mT. From Ref. 35, with permission.

II-H. Pheophytin radical

Ph^- can be generated in the absence of Q_A^- by illuminating Photosystem II membranes in the presence of dithionite, as above, but at room temperature. Under these conditions, Q_A^- appears to undergo photoreduction to the diamagnetic Q_AH_2 state, and Ph^- is produced as well, as above [35,86]. Ph^- is also observed in the presence of dithionite in D1/D2/cytochrome *b*-559 preparations, which lack Q_A and Q_B altogether [10,84,87]. Thus, simple Ph^- can be trapped and observed. The Ph^- EPR signal is centered at $g = 2.0035$ with a width of $\Delta H = 1.25$ mT [86] (and see Ref. 88 for the bacterial signal).

II-I. Tyrosine Y_Z^+ radical

Ph^- is currently the earliest discrete component of the electron acceptance chain that can be observed in its photoreduced state. However, a couple of early electron donors with very short-lived oxidized states remain to be described. These are the tyrosine residue that mediates electron transfer from the Mn complex to the primary electron donor, Y_Z, and the primary electron donor itself (Scheme II).

When the Mn complex has been inactivated, or electron transport between it and Y_Z is blocked, a steady-state population of Y_Z^+ can accumulate and be observed during intense illumination at room temperature (signal II_f) (see Ref. 89, and recently, Ref. 90). The EPR signal of Y_Z^+ has the same lineshape as that of Y_D^+ (see Fig. 1, subsection II-A), and indeed, Y_Z^+ has been shown to be a tyrosine radical analogous to Y_D^+ by EPR spectroscopy of mutant *Synechocystis* (Y_Z = Tyr-161 of D1) [91,92]. In intact Photosystem II, the Mn complex rereduces Y_Z^+ so quickly that Y_Z^+ is too short-lived to be observable by EPR without heroic effort (signal II_{vf}) [93]. Nonetheless, the time constants for the appearance and disappearance of the EPR signal of Y_Z^+ have been measured to obtain the oxidation and rereduction rates of Y_Z in intact and disrupted Photosystem II (reviewed in Ref. 6).

II-J. The primary electron donor: P680$^+$

The primary electron donor in Photosystem II is named P680, in reference to its absorption maximum of 680 nm (P680 = *p*igment absorbing at 680 nm). In order to observe $P680^+$ by EPR, it is necessary to prevent its rereduction by all three electron donation paths (Scheme II), as well as recombination of $P680^+$ with reduced electron acceptors. Therefore, $P680^+$ is difficult to observe. The Chl^+ EPR signal (subsection II-F) has, in the past, been ascribed both to a Chl electron donor to $P680^+$ and to $P680^+$ itself (discussed by Lozier and Butler [94]). Visser and Rijgersberg [81] and Malkin and Bearden [95], however, appear to have been observing $P680^+$ as well as Chl^+, under oxidizing conditions. Similarly, Nugent et al. observed $P680^+$ and Chl^+ together in D1/D2/cytochrome *b*-559 preparations [84]. More recent reports of $P680^+$ EPR signals have combined the use of inhibitory conditions and rapid time-resolved methods of detection to discriminate between $P680^+$ and other species. Thus, in the presence of inhibitors known to slow electron donation in Photosystem II, Ghanotakis and Babcock [96] and Bock et al. [97] obtained EPR signals ascribed to $P680^+$ which were very similar to the signal of Chl^+, but which decayed with a half time of 200 μs or less at 273 K [97]. The EPR signal of $P680^+$ has the same *g* value as that of Chl^+ ($g = 2.0025$), but has a smaller linewidth of only $\Delta H = 0.7$–0.9 mT [98]. Nonetheless, it is not yet certain whether P680 is a Chl dimer or a monomer (see the discussion in Refs. 99, 100 and below, and see Ref. 7, for the bacterial primary electron donor).

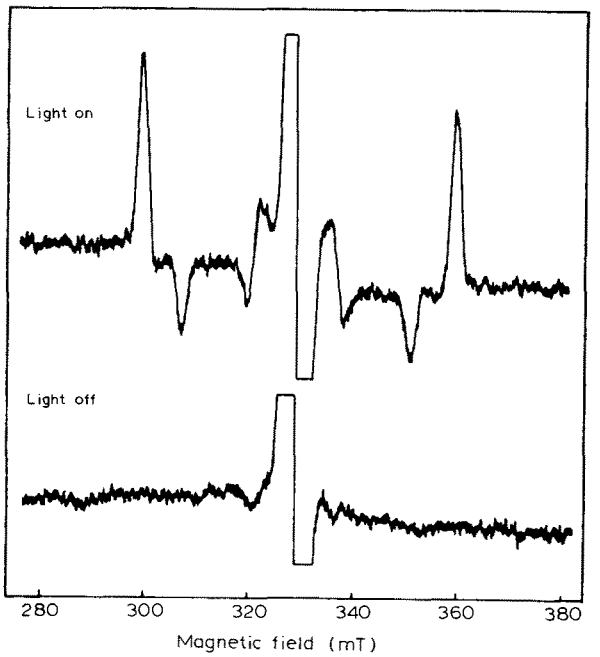

Fig. 6. The spin-polarized triplet P680 signal. The signal of ^{3}P680 may be observed ('Light on') during illumination at 3–5 K of Photosystem II particles containing Q_AH_2 (here resulting from the detergent treatment used, and reduction with sodium dithionite, see [101]). In contrast, the triplet signal is absent from a spectrum obtained in darkness from the same material ('Light off'). The samples were suspended in ethylene glycol-free medium. Instrument conditions: sample temperature, 3–5 K; microwave power, 10 μW; microwave frequency, 9.26 GHz; magneitc field modulation amplitude, 1.0 mT. From Ref. 101, with permission.

II-K. Triplet P680

An EPR signal from triplet P680 has also been observed (Fig. 6, from Ref. 101). This species is deemed to result from recombination of $P680^+$ and Ph^- (Scheme II), as does a similar triplet signal produced in bacterial reaction centers [102]. The signal is centered at $g \approx 2$ and extends over approx. 60 mT [101]. Thurnauer et al. [103] have explained the *aeeaae* pattern of the bacterial signal as indicative of recombination between two separated spins that have not depolarized (a = absorption, e = emission). Although the D and E values of the triplet signal of Photosystem II are similar to those of monomeric Chl triplet ($D = 0.027$–0.029 cm^{-1} and $E = 0.0039$–0.0040 cm^{-1}), they could also arise from a Chl dimer under certain conditions [99,101]. If, indeed, this triplet does correspond to ^{3}P680 [104], then its orientation with respect to the thylakoid membrane plane [40] suggests that the arrangement of P680 in the reaction center of Photosystem II is very different from that of the primary electron donor in the bacterial reaction center [105]. Alternatively, the triplet may reside on one of the accessory Chl molecules in the Photosystem II reaction center [105].

The triplet signal ascribed to P680 is observed best when Q_A is doubly reduced to Q_AH_2 [106], or absent, as in D1/D2/cytochrome *b*559 preparations [107]. In these cases, there is no electrostatic repulsion between Q_A^- and Ph^- to inhibit formation of the $P680^+$ Ph^- radical pair that gives rise to the triplet [106] and, at the same time, electron transfer beyond Ph^- is impossible. In addition, inhibition of electron donation to $P680^+$, by illumination at extremely low temperatures, favors recombination between $P680^+$ and Ph^-. Finally, the signal is observed during illumination, because the triplet decays with a half-life of approx. 1 ms at liquid He temperatures [106]. Thus, spectra are collected during illumination, from Photosystem II that has been treated with reductant, at temperatures of 3–5 K, to produce a steady-state population of the triplet (see Ref. 105).

In summary, Q_A^-, (Q_B^-), Ph^-, Y_D^+, the S_2 state of the Mn complex, oxidized cytochrome *b*-559 and Chl^+ can be trapped after illumination for later study by EPR. In Photosystem II membranes, shorter-lived species such as Y_Z^+ and ^{3}P680 can be observed during intense illumination, in conjunction with treatments that inhibit later electron transport steps, and thus enhance accumulation of steady-state populations of the paramagnetic species. Y_Z^+, and the even shorter-lived $P680^+$, have also been detected as transients after saturating illuminating flashes, by time-resolved EPR methods. Thus, combinations of illumination, selective inhibition and transient methods have permitted observation of all the currently recognized electron transport components of Photosystem II by EPR.

II-L. The quinone-ferric iron complex: $Fe^{3+}Q_A$

Certain chemical treatments result in an alternative state of the FeQ_A electron acceptor complex of Photosystem II: $Fe^{3+}Q_A$. This species, sometimes called Q-400 (fluorescence *Q*uencher with a reduction potential of 400 mV), is occasionally observed at high microwave observation power and low temperature (20–50 mW, 4–5 K; reviewed in Ref. 108). It can be generated by briefly annealing a sample containing PPBQ (a two electron acceptor) at 273 K, after illuminating it at 200 K or lower [46,109]. The illumination generates $Fe^{2+}Q_A^-$, which is chemically oxidized to $Fe^{3+}Q_A$ by PPBQ during annealing (Fig. 7a). Alternatively, chemical oxidation alone, with $Fe(CN)_6^{3-}$, will also work [110]. $Fe^{3+}Q_A$ can be photochemically rereduced, to give $Fe^{2+}Q_A$ and then $Fe^{2+}Q_A^-$. Thus, in a series of flashes of light, the amplitude of the $Fe^{3+}Q_A^-$ signal oscillates, as Fe^{2+} is first oxidized, and then photoreduced, on alternate flashes [46].

Higher pH levels [110], and removal of a 28 kDa polypeptide [111] facilitate production of $Fe^{3+}Q_A$ (Fig. 7b). The turning points of the $Fe^{3+}Q_A$ signal occur at $g = 8$ and 5.5 [110,46], however, shifts in g values

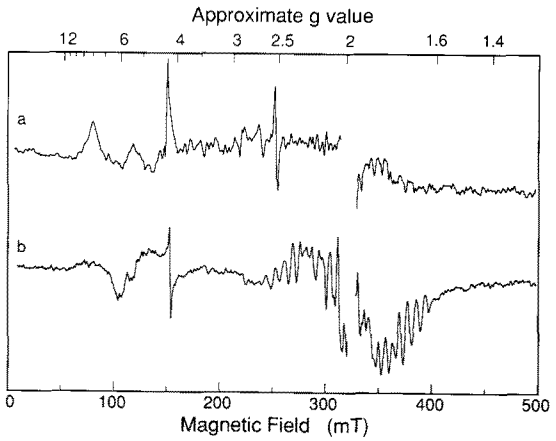

Fig. 7. The $Fe^{3+}Q_A$ EPR signal. (a) Generated by illumination at 77 K and annealing with PPBQ at 273 K. In this case, a sample of Photosystem II membranes containing 0.4 M sucrose as the cryoprotectant and PPBQ was illuminated at 77 K for 10 min, and then annealed at 273 K for 15 s. The (annealed-illuminated) difference spectrum shows the appearance of two peaks with $g \approx 8$ and 5.5 due to $Fe^{3+}Q_A$, and the disappearance of the signal from $Fe^{2+}Q_A^-$ (see Fig. 2) upon annealing (courtesy of J.B. Innes). An artifact of subtraction of the rhombic Fe signal ($g \approx 4.2$), (as well as a small signal from O_2 at $g \approx 2.5$) are also present. (b) The inverse of the $Fe^{3+}Q_A$ signal may be observed in Photosystem II membranes suspended in 30% ethylene glycol with 0.1 mM DCMU. After treatment with 1 M $CaCl_2$ to deplete certain polypeptide constituents of Photosystem II [83], $Fe^{3+}Q_A$ may be present in the dark, and become reduced upon illumination (at 200 K for 4 min), so that the $Fe^{3+}Q_A$ signal disappears. In such cases, the illuminated-minus-dark difference spectrum contains a negative signal from $Fe^{3+}Q_A$ ($g \approx 7$ and 6, due to DCMU), as well as the S_2-state multiline signal ($g \approx 2$, $a \approx 8.5$ mT) and underlying $Fe^{2+}Q_A^-$ signals. Instrument conditions: (a) sample temperature, 4.5 K; microwave power, 22 mW; (b) sample temperature, 7.5 K; microwave power, 0.2 mW; all other parameters as in Fig. 3.

indicative of an increase in axial symmetry are observed in the presence of certain inhibitors that bind to Photosystem II in the Q_B-binding site [112]. For example, in the presence of DCMU, turning points are observed at $g \approx 7$ and 6 (Fig. 7b), instead of the $g \approx 8$ and 5.5 turning points that are observed in the presence of ferricyanide alone [108]. The EPR signal of $Fe^{3+}Q_A$ and its temperature dependence are consistent with high spin Fe^{3+} with $D = 1.0\ cm^{-1}$ and $E/D = 0.1$ [108,113]. Furthermore, the spectral characteristics of the Fe^{3+} signal have been interpreted to suggest ligation by bicarbonate or tyrosine, as well as histidine [113].

Coordination of NO to the Fe^{2+} and perturbation of the FeQ_A site has also recently been reported, along with another EPR signal, from $Fe^{2+}NO$ ($g_\perp = 4.2$, $S = \frac{3}{2}$) [114].

II-M. The g = 2, 16 mT-wide signal

Recently, work on Ca^{2+}-depleted Photosystem II membranes has revealed another EPR signal with $g \approx 2$, and a linewidth of approx. 16 mT [57,59]. This signal is formed upon illumination, at approx. 273 K, of Ca^{2+}-depleted Photosystem II membranes, initially in a state corresponding to S_2. Therefore, this signal has been associated with a state corresponding to S_3, and possibly an intermediate in the S-state cycle [57]. Based on its g value of approx. 2, in combination with its extremely large linewidth and the low temperatures or high microwave powers required to saturate it, this signal has been attributed to a free radical (possibly an oxidized protein residue) in magnetic contact with a metal center (the Mn complex) [57,59]. Specifically, Boussac et al. have proposed that the 16 mT-wide signal originates from photooxidized histidine coupled to the Mn complex, and that a similar species is formed in the normal S_3 state of Photosystem II [115].

Nonetheless, the significance of this signal remains unclear. It is of note that a possibly unrelated signal, that nonetheless displays a similar lineshape, has been reported in NH_2OH-treated and Tris-washed Photosystem II membranes [116,117].

III. EPR signals from components of the cytochrome b_6f and Photosystem I complexes

EPR spectroscopy is sufficiently sensitive that micromolar contaminants may be visible, and occasionally, Photosystem II membrane preparations contain other thylakoid membrane components (Scheme I). Of these, the cytochrome b_6f complex is the most common impurity in Photosystem II membrane preparations because it is more closely associated with the stacked regions of thylakoid membranes where Photosystem II is concentrated. Collectively, the components of the cytochrome b_6f complex act to couple electron transfer between Photosystem II and Photosystem I to H^+ translocation across the thylakoid membrane, and thus to sustain a transmembrane proton gradient.

III-A. Cytochromes

In EPR spectra collected at approx. 10 K, one can sometimes see signals from oxidized high-spin cytochrome b_6 (= cytochrome b-563) at $g_\perp \approx 6$ (Figs. 3, 8, 9). This signal represents non-native configurations [118], and their high-spin ($S = \frac{5}{2}$) state results from loss of one of the heme iron's six ligands. The $g_\perp$ value of 6 is characteristic of $S = \frac{5}{2}$ species with axial symmetry for which only the $m_s = \pm\frac{1}{2}$ levels are populated, due to large zero-field splitting (D). Thus, other disrupted cytochromes also have signals in this region, but cytochrome b_6 is particularly labile and, therefore, a common source of the signal at $g \approx 6$ [118,119]. Furthermore, unlike $Fe^{3+}Q_A$, which occurs in the same spectral region, oxidized disrupted cytochrome b_6 is not photochemically active at low temperatures, so the $g \approx 6$ cytochrome signal does not disappear upon illumination at temperatures of less than approx. 200 K. Both the

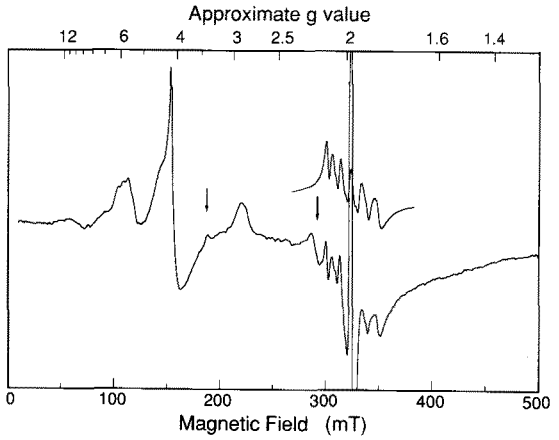

Fig. 8. Low-potential cytochrome *b*-559 and $Mn^{2+}(H_2O)_6$. Treatments that release the extrinsic polypeptides cause conversion of cytochrome *b*-559 to its lower-potential forms and destabilize the Mn complex. A spectrum of dark-adapted Photosystem II membranes treated with 1 M $CaCl_2$ to release all three extrinsic polypeptides [83] shows the six-lined $Mn^{2+}(H_2O)_6$ signal with $g = 2.0$ and $a = 9.5$ mT (275–350 mT) due to approx. 0.3 Mn per Photosystem II center. Also evident are low-potential cytochrome *b*-559 with $g_z \approx 3$ and $g_y \approx 2.2$, contributions from high-spin oxidized cytochrome contaminants and some $Fe^{3+}Q_A$ at $g \approx 6$, rhombic Fe^{3+} ($g = 4.2$), oxidized cytochrome *f* at $g \approx 3.5$ and Y_D^+ ($g = 2.0$, off scale). Arrows indicate the $g_y = 2.2$ turning point of cytochrome *b*-559 and the $g_z \approx 3.5$ turning point of cytochrome *f*. The signal of excess Mn^{2+} (0.2 mM) added to NH_2OH-treated Photosystem II membranes [148,149] is also shown as an inset, scaled to the same size, for comparison. The NH_2OH treatment reduces Y_D^+, so that signal is absent. Instrument conditions: sample temperature for full spectrum, 7.5 K; sample temperature for inset, 10 K; all other parameters as in Fig. 3.

lineshapes and g values of high-spin photosynthetic cytochromes appear to be somewhat variable, for example during the course of a redox titration [119]. Published g values range from 5.4 to 7.2 [74,120].

In their native, 6-coordinate, low-spin configurations, oxidized cytochromes *f* and b_6 have turning-points at $g_z = 3.51$ and $g_z = 3.6$, respectively [118,119] (for example, see Fig. 8). These signals are rarely seen in Photosystem II membrane preparations, however, least of all that of cytochrome b_6, which is broad. EPR signals from cytochrome *f* (or b_6) contaminants may appear in spectra of dark-adapted samples of Photosystem II membranes. However, the signals can disappear upon illumination and reduction of the cytochromes by electrons from Photosystem II, unless DCMU or low illumination temperature block electron transfer between Q_A and Q_B. For spectra of cytochrome b_6f preparations, see Rich et al. [119].

III-B. The Rieske iron-sulfur center

The Rieske iron-sulfur center is a Fe_2S_2 cluster present in the cytochrome b_6f complex. The reduced ($Fe^{2+}Fe^{3+}$) state is visible by EPR. Therefore, in thylakoid membranes, the EPR signal of the Rieske iron-sulfur center will tend to increase in amplitude as a result of electron transfer from Photosystem II (at temperatures above 230 K), but decrease in amplitude as a result of oxidation by Photosystem I, via plastocyanin (Scheme I). The g values of the Rieske Fe_2S_2 center are $g_z = 2.02$, $g_y = 1.89$ and $g_x = 1.78$ (reviewed in Ref. 121), but the appearance of the Rieske iron-sulfur center signal is sensitive to effects at the quinol-binding site [122]. The turning point one tends to notice in spectra of Photosystem II membranes is g_y [123] (Figs. 3a and 4a).

III-C. The primary electron donor: $P700^+$, and triplet P700

Contamination of Photosystem II membranes by Photosystem I is also possible, although less likely than contamination with the cytochrome b_6f complex. Photosystem I effects the final light-driven electron transfer steps that result in production of NADPH (see Scheme I). Electron transport and the components of Photosystem I have been reviewed by Rutherford and Heathcote [124].

EPR signal I from Photosystem I figured in the first report of biological EPR signals [125], hence its name. This signal has since been identified with the primary electron donor of Photosystem I, $P700^+$ [126], and resembles the Chl^+ signal (Fig. 1) with $g = 2.0026$, but a width of $\Delta H = 0.74$ mT [21,22].

$P700^+$ is completely rereduced within seconds of photooxidation at room temperature, much faster than is Y_D^+. Therefore, it is possible to obtain a spectrum of Y_D^+ without interference from $P700^+$, to use as a spin standard, by delaying approx. 10 s after illumination, before trapping at 77 K. Furthermore, P700 can be chemically oxidized by $K_3Fe(CN)_6$. Therefore, the extent of Photosystem I contamination in a preparation of Photosystem II membranes can be estimated by comparing a spectrum of $K_3Fe(CN)_6$-oxidized material with a spectrum of untreated material, after both samples have been illuminated and then frozen after a short dark interval. Y_D^+ should be produced quantitatively in both cases, with additional quantitative production of $P700^+$ in the chemically-oxidized sample only.

Finally, the EPR signal of triplet P700 has also been observed, with D and E values close to those expected for monomeric Chl [127]. The $^3P700$ signal is slightly narrower than that of $^3P680$ (compared in Ref. 128). Although the optical spectrum of P700 indicates that P700 is a Chl dimer in the ground state, the unpaired electron of $P700^+$ and the triplet state of P700 may be localized on only one of the two Chl moieties (see discussions in Refs. 4, 5).

III-D. Early electron acceptors A_0 and A_1

EPR signals have been attributed to the primary electron acceptors of Photosystem I, A_0 and A_1, but these are not too likely to appear accidentally in an EPR spectrum of Photosystem II membranes. This is because one must either remove, or reduce the iron-sulfur centers of Photosystem I, in order to prevent them from rapidly reoxidizing photoreduced A_0 and A_1. However, this can be done, for example, by multiple turnovers in the presence of dithionite (see Scheme I, reviewed in Ref. 4). Based on optical spectroscopy and the EPR characteristics of A_0 ($g = 2.002$ and $\Delta H = 1.15$ mT [124]), A_0 has been tentatively identified as a Chl anion radical. A_1 has been identified as phylloquinone (vitamin K) by inactivation and reconstitution experiments [129–130]. However, the EPR signal initially associated with A_1 ($g = 2.0054$ and $\Delta H = 1.1$ mT [124]) is now thought to arise from some other species [131,132].

III-E. Fe_4S_4 centers of Photosystem I

The terminal electron acceptors in Photosystem I are Fe_4S_4 centers, called F_A and F_B (not necessarily functioning in series). A third Fe_4S_4 center, called F_X and contained in the Photosystem I core, may serve as an intermediate electron acceptor (Scheme I; reviewed in Ref. 124 and see Ref. 133). The Fe_4S_4 centers are photoreduced, and thus visible by EPR, after illumination and/or chemical reduction to $Fe^{3+}Fe_3^{2+}$. Within each cluster, the Fe ions are exchange coupled, with both ferromagnetic and antiferromagnetic pairwise interactions [134], with the net effect that the clusters are $S = \frac{1}{2}$ species in the state observed by EPR. Their distorted octahedral symmetries result in three turning points for each center, the g values of which are used to identify the Fe_4S_4 cluster producing the EPR signal. (Fe_4S_4 center F_A has $g_x = 2.05$, $g_y = 1.95$ and $g_z = 1.86$; Fe_4S_4 center F_B has g values of $g_x = 2.06$, $g_y = 1.90$ and $g_z = 1.89$; and Fe_4S_4 center F_X has $g_x = 2.06$, $g_y = 1.86$ and $g_z = 1.76$ (Refs. 7, 124 and references therein).) However, the Fe_4S_4 centers are close enough to interact with one another magnetically. As a result, reduction of F_B in the presence of reduced F_A causes F_A's $g_z = 1.86$ turning point to disappear. Spectra of the Fe_4S_4 clusters are shown in Ref. 135 and their orientation dependences have been characterized [122,136]. Malkin and Bearden [121] have reviewed chloroplast iron-sulfur proteins.

IV. EPR signals from contaminating metal ions and O_2

IV-A. Rhombic Fe^{3+}

The contaminating signal that is most often observed in Photosystem II membranes (essentially always, at liquid He temperatures) is that of rhombic Fe^{3+} impurities ($S = \frac{5}{2}$, Fig. 3a,b, 8 and 9b,c). The rhombic Fe^{3+} signal is asymmetric, approx. 20 mT wide and has a g value of $g = 4.2$, which has been explained by Aasa [137]. The source of many a subtraction artifact (Fig. 7a, b), the sharp peak of this signal can also be useful for aligning spectra. One common cause of subtraction artifacts in difference spectra is acquisition of the pre- and post-illumination spectra at slightly different temperatures, leading to greater rhombic Fe^{3+} signal amplitude in the spectrum collected at the lower temperature, as a result of this signal's temperature dependence.

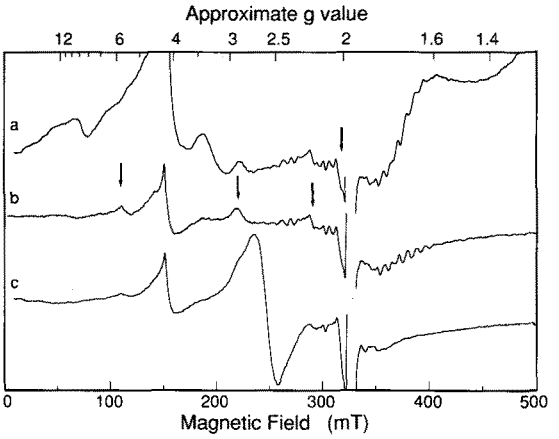

Fig. 9. Selected interfering signals from O_2. (a) The contributions of O_2 to an especially ugly spectrum of Photosystem II membranes (collected after illumination at 200 K) can be eliminated by purging the EPR cryostat with N_2 at 200 K with the sample in place, to yield spectrum (b). EPR signals from O_2 can appear as a result of reorganization or condensation of O_2 in or on a sample tube, in the course of manipulations. Spectrum (c) shows a large signal, most probably from O_2, at $g \approx 2.6$. (This spectrum was obtained from Mn- and extrinsic polypeptide-depleted Photosystem II membranes, after illumination at 273 K.) Also apparent are the signal from Rhombic Fe^{3+} at $g = 4.2$ (a, b, c), the S_2-state multiline signal (a, b) and the underlying $Fe^{2+}Q_A^-$ signals (b, c). Arrows indicate the signals from non-native configurations of cytochromes at $g_\perp \approx 6$ (b), low-potential cytochrome *b*-559 at $g \approx 3$ and 2.2 (a, b, c) and Cu^{2+} at $g_\perp = 2.05$ (a, b, c). Instrument conditions as in Fig. 3.

IV-B. Cu^{2+}

Cu^{2+} is almost always observed in Photosystem II membrane preparations, with $g_\perp = 2.05$, mainly at liquid He temperatures (Figures 4a, 9b). It is unlikely that plastocyanin, a soluble Cu^{2+}-containing electron transport protein (Scheme I), would be retained in the many washes used to prepare Photosystem II membranes. A more plausible source of Cu^{2+} is the light-harvesting complex of Photosystem II [138]. Cu^{2+} is a d^9 ion ($S = \frac{1}{2}$), which frequently adopts square planar symmetry in proteins. The two distinct g values can usually be resolved, as well as the parallel component of the hyperfine splitting. For example, plastocyanin has $g_\perp = 2.05$, $g_\parallel = 2.24$ and $a_\parallel = 60$ mT [139,140]. EPR spectra of Cu^{2+} can be quite informative because they can exhibit

well-resolved superhyperfine couplings to N or F ligands, and the Cu^{2+} g and a values are diagnostic of the structure and ligation of the Cu^{2+} center (reviewed in Ref. 141).

IV-C. Mn^{2+}

The six-line EPR signal of hexaaquo Mn^{2+} is often visible, at $g = 2.00$, with $a = 9.5$ mT, from liquid He to room temperatures (Fig. 8). The signal is isotropic because it arises from a high-spin ($S = \frac{5}{2}$) d^5 Mn^{2+} ion with one electron in each d orbital in an approximately octahedral crystal field (and thus with a symmetric distribution of electron density). The six lines of the $Mn^{2+}(H_2O)_6$ EPR signal arise from hyperfine coupling with the six possible values of the ^{55}Mn nuclear spin ($I = \frac{5}{2}$), and each line represents five almost degenerate spin transitions ($m_s = \frac{5}{2} \leftrightarrow \frac{3}{2}$, $\frac{3}{2} \leftrightarrow \frac{1}{2}$, $\frac{1}{2} \leftrightarrow -\frac{1}{2}$, $-\frac{1}{2} \leftrightarrow -\frac{3}{2}$ and $-\frac{3}{2} \leftrightarrow -\frac{5}{2}$). However, for Mn^{2+} which is bound in an asymmetric environment, in slowly-tumbling proteins, separation of the different m_s levels, and the orientation-dependence of the transitions among them, lead to numerous broad signal components. In extreme cases, only the $m_s = \frac{1}{2} \leftrightarrow -\frac{1}{2}$ transitions remain resolvable, so the simple familiar six-line signal is observed (somewhat narrower than the fivefold degenerate signal), but with the intensity reduced by as much as a factor of four (see Ref. 142). The main source of Mn^{2+} in thylakoids is adventitious Mn^{2+} [143]. This can be displaced by washing with buffers containing 5 mM Ca^{2+} or Mg^{2+} (and 1 mM EDTA). Thus, adventitious Mn^{2+} should be negligible in most Photosystem II membrane preparations. The other common source of Mn^{2+} is denaturation of the Mn complex of Photosystem II. Therefore, an increase in the level of hexaaquo Mn^{2+} after a treatment bodes ill for the integrity of the Mn complex and O_2-evolution activity. One can use the EPR signal of hexaaquo Mn^{2+} to quantitate the total Mn content of Photosystem II membranes, after treating a sample with HCl (0.5 M final), to free all the Mn as Mn^{2+}, and protonate all chelating groups [143].

IV-D. O_2

O_2 signals are very frustrating additions to almost any spectrum because they may appear or disappear in the course of illumination or annealing treatments. This results in large signals in the difference spectra, which appear to be responsive to the treatment. Indeed, there have been several published reports in which EPR signals that are now believed to have been due to O_2 were attributed to Photosystem II.

O_2 is a triplet with rotational as well as spin and orbital angular momentum. Some 120 different EPR spectral lines are predicted and observed for gaseous O_2 [144,145] (see Ref. 146 for figures). In addition, intermolecular ferromagnetic interactions complicate the situation and lead to the formation of spin domains when O_2 is fairly concentrated (condensed on the surface of a sample, in bubbles in a sample, or trapped in frost on the outside of sample tubes). Therefore, the low temperature EPR spectrum of O_2 contains an extremely wide range of components whose contributions may vary (for example, compare Fig. 9a with 9c). Furthermore, cooling samples in a strong magnetic field, and thus with the spins of O_2 aligned, can trap O_2 in the conformations associated with this alignment and preserve its strongly oriented character. In such a case, because O_2's EPR signals are anisotropic, a small change in sample orientation may cause signal intensity to appear in different positions in successive spectra, and lead to subtraction artifacts. As a result, it is important to purge O_2 from the EPR cryostat and cavity, and keep EPR tubes free of frost (Fig. 9b). Persistent O_2 signals (Fig. 9c) can usually be eliminated by thawing the sample and vigorously shaking it down in the EPR tube to remove all bubbles. Finally, the top surface of the sample in the EPR tube should be positioned above the sensitive volume of the EPR cavity, so that any O_2 that condenses onto the sample will not be detected. Fortunately, signals from O_2 are only readily observed at liquid He temperatures.

V. Concluding remarks

EPR spectroscopy is a sensitive and informative probe of photosynthetic electron transport. It has contributed important insights into Photosystem II as an analytical technique, a method for identifying the chemical natures and roles of various species, and a means of monitoring the competing paths and rates of electron transfer. This method is now being extended in such forms as electron spin echo spectroscopy and electron nuclear double resonance spectroscopy, and continues to augment our understanding of electron transfer processes and biochemistry in general.

Acknowledgements

This work was supported by the National Institutes of Health (GM32715). GWB is the recipient of a Camille and Henry Dreyfus Teacher/Scholarship. The authors would like to thank J.B. Innes for an EPR spectrum and A.W. Rutherford for helpful discussions, a preprint of a paper in press and permission to use two figures from his published work in this review.

References

1 Knowles, P.F., Marsh, D. and Rattle, H.W.E. (1976) Magnetic Resonance of Biomolecules, John Wiley & Sons, New York.
2 Wertz, J.E. and Bolton, J.R (1986) Electron Spin Resonance, Chapman & Hall.
3 Hoff, A.J. (1987) in New Comprehensive Biochemistry: Photosynthesis (Amesz, J., ed.), pp. 97–123, Elsevier, Amsterdam.

4 Andréasson, L.-E. and Vänngård, T. (1988) Annu. Rev. Plant Physiol. Plant Mol. Biol. 39, 379–411.
5 Mathis, P. and Rutherford, A.W. (1987) in New Comprehensive Biochemistry: Photosynthesis (Amesz, J., ed.), pp. 63–96, Elsevier, Amsterdam.
6 Babcock, G.T. (1987) in New Comprehensive Biochemistry: Photosynthesis (Amesz, J., ed.), pp. 125–158, Elsevier, Amsterdam.
7 Okamura, M.Y., Feher, G. and Nelson, N. (1982) in Photosynthesis: Energy Conversion by Plants and Bacteria, I (Govindjee, ed.), pp. 195–272, Academic Press, N.Y.
8 Dutton, P.L., Prince, R.C. and Tiede, D.M. (1978) Photochem. Photobiol. 28, 939–949.
9 Rutherford, A.W. (1987) in Progress in Photosynthesis Research (Biggins, J., ed.), Vol. I, pp. 277–283, Martinus Nijhoff/Dr. Junk, Dordrecht.
10 Nanba, O. and Satoh, K. (1987) Proc. Natl. Acad. Sci. USA 84, 109–112.
11 Michel, H. and Deisenhofer, J. (1988) Biochemistry 27, 1–7.
12 Berthold, D.A., Babcock, G.T. and Yocum, C.F. (1981) FEBS Lett. 134, 231–234.
13 Beck, W.F., De Paula, J.C. and Brudvig, G.W. (1985) Biochemistry 24, 3035–3043.
14 Thompson, L.K., Miller, A.-F., De Paula, J.C. and Brudvig, G.W. (1988) Isr. J. Chem. 28, 121–128.
15 Buser, C.A., Thompson, L.K., Diner, B.A. and Brudvig, G.W. (1990) Biochemistry 29, 8977–8985.
16 Debus, R.J., Barry, B.A., Babcock, G.T. and McIntosh, L. (1988) Proc. Natl. Acad. Sci. USA 85, 427–430.
17 Vermaas, W.F.J., Rutherford, A.W. and Hansson, Ö. (1988) Proc. Natl. Acad. Sci. USA 85, 8477–8481.
18 Styring, S. and Rutherford, A.W. (1987) Biochemistry 26, 2401–2405.
19 Vermaas, W.F.J., Renger, G. and Dohnt, G. (1984) Biochim. Biophys. Acta 764, 194–202.
20 Babcock, G.T. and Sauer, K. (1973) Biochim. Biophys. Acta 325, 483–503.
21 Kohl, D.H. (1972) in Biological Applications of ESR (Schwartz, H.M., Bolton, J.R. and Borg, D.C., eds.), pp. 213–264, Wiley & Sons, New York.
22 Weaver, E.C. and Corker, G.A. (1977) in the Encyclopedia of Plant Physiology, Vol. 5: Photosynthesis, I (Trebst, A. and Avron, M., eds.), pp. 168–178, Springer, Berlin.
23 Commoner, B., Heise, J.J. and Townsend, J. (1956) Proc., Natl. Acad. Sci. USA 42, 710–718.
24 Babcock, G.T., Barry, B.A., Debus, R.J., Hoganson, C.W., Atamian, M., McIntosh, L., Sithole, I. and Yocum, C.F. (1989) Biochemistry 28, 9557–9565.
25 Barry, B.A. and Babcock, G.T. (1987) Proc. Natl. Acad. Sci. USA 84, 7099–7103.
26 Petersen, J., Dekker, J.P., Bowlby, N.R., Ghanotakis, D.F., Yocum, C.F. and Babcock, G.T. (1990) Biochemistry 29, 3226–3231.
27 Styring, S. and Rutherford, A.W. (1988) Biochemistry 27, 4915–4923.
28 Babcock, G.T., Ghanotakis, D.F., Ke, B. and Diner, B.A. (1983) Biochim. Biophys. Acta 723, 276–286.
29 De Paula, J.C., Innes, J.B. and Brudvig, G.W. (1985) Biochemistry 24, 8114–8120.
30 Vass, I., Deák, Z., Jegerschöld, C. and Styring, S. (1990) Biochim. Biophys. Acta 1018, 41–46.
31 Kawamori, A., Satoh, J., Inui, T. and Satoh, K. (1987) FEBS Lett. 217, 134–138.
32 Nugent, J.H.A., Demetriou, C. and Lockett, C.J. (1987) Biochim. Biophys. Acta 894, 534–542.
33 Deisenhofer, J., Epp, O., Miki, K., Huber, R. and Michel, H. (1985) Nature 318, 618–624.
34 Nugent, J.H.A., Diner, B.A. and Evans, M.C.W. (1981) FEBS Lett. 124–241–244.
35 Rutherford, A.W. and Zimmermann, J.-L. (1984) Biochim. Biophys. Acta 767, 168–175.
36 Vermaas, W.F.J. and Rutherford, A.W. (1984) FEBS Lett. 175, 243–248.
37 Rutherford, A.W., Zimmermann, J.-L. and Mathis, P. (1984) FEBS Lett. 165, 156–162.
38 Leigh, J.S. and Dutton, P.L. (1972) Biochem. Biophys. Res. Commun. 46, 414–421.
39 Butler, W.F., Calvo, R., Fredkin, D.R., Isaacson, R.A., Okamura, M.Y. and Feher, J. (1984) Biophys. J. 45, 947–973.
40 Rutherford, A.W. (1985) Biochim. Biophys. Acta 807, 189–201.
41 Klimov, V.V., Dolan, E., Shaw, E.R. and Ke, B. (1980) Proc. Natl. Acad. Sci. USA 77, 7227–7231.
42 Debus, R.J., Feher, G. and Okamura, M.Y. (1986) Biochemistry 25, 2276–2287.
43 Wraight, C.A. (1978) FEBS Lett. 93, 283–288.
44 Beijer, C. and Rutherford, A.W. (1987) Biochim. Biophys. Acta 890, 169–178.
45 Rutherford, A.W., Zimmermann, J.-L. and Mathis, P. (1984) in Advances in Photosynthesis Research (Sybesma, C., ed.), Vol. I, pp. 445–448, Martinus Nijhoff/Dr. Junk, Dordrecht.
46 Zimmermann, J.-L. and Rutherford, A.W. (1986) Biochim. Biophys. Acta 851, 416–423.
47 Kok, B., Forbush, B. and McGloin, M. (1970) Photochem. Photobiol. 11, 457–475.
48 Dismukes, G.C. and Siderer, Y. (1981) Proc. Natl. Acad. Sci. USA 78, 274–278.
49 Brudvig, G.W., Casey, J.L. and Sauer, K. (1983) Biochim. Biophys. Acta 723, 366–371.
50 Styring, S. and Rutherford, A.W. (1988) Biochim. Biophys. Acta 933, 378–387.
51 Hansson, Ö., Aasa, R. and Vänngård, T. (1987) Biophys. J. 51, 825–832.
52 Haddy, A., Aasa, R. and Andréasson, L.-E. (1989) Biochemistry 28, 6954–6959.
53 Hansson, Ö., Andréasson, L.-E. and Vänngård, T. (1986) FEBS Lett. 195, 151–154.
54 Beck, W.F., De Paula, J.C. and Brudvig, G.W. (1986) J. Am. Chem. Soc. 108, 4018–4022.
55 Andréasson, L.-E. and Hansson, Ö. (1987) in Progress in Photosynthesis Research (Biggins, J., ed.), Vol. I, pp. 503–510, Martinus Nijhoff/Dr. Junk, Dordrecht.
56 Britt, R.D., Zimmermann, J.L., Sauer, K. and Klein, M.P. (1989) J. Am. Chem. Soc. 111, 3522–3532.
57 Boussac, A., Zimmermann, J.-L. and Rutherford, A.W. (1989) Biochemistry 28, 8984–8989.
58 Ono, T. and Inoue, Y. (1989) Physiol. Plant. 76, A141.
59 Sivaraja, M., Tso, J. and Dismukes, G.C. (1989) Biochemistry 28, 9459–9464.
60 Boussac, A. and Rutherford, A.W. (1988) Biochemistry 27, 3476–3483.
61 Rutherford, A.W. (1989) Trends Biochem. Sci. 14, 227–232.
62 Pecoraro, V.L. (1988) Photochem. Photobiol. 48, 249–264.
63 Arnold, W. and Clayton, R.K. (1960) Proc. Natl. Acad. Sci. USA 46, 769–776.
64 Zimmermann, J.-L. and Rutherford, A.W. (1986) Biochemistry 25, 4609–4615.
65 Casey, J.L. and Sauer, K. (1984) Biochim. Biophys. Acta 767, 21–28.
66 Ono, T., Zimmermann, J.-L., Inoue, Y. and Rutherford, A.W. (1986) Biochim. Biophys. Acta 851, 193–201.
67 Beck, W.F. and Brudvig, G.W. (1988) Chim. Scr. 28A, 93–98.
68 Dismukes, G.C. (1988) Chim. Scr. 28A, 99–104.
69 Yachandra, V.K., Guiles, R.D., Sauer, K. and Klein, M.P. (1986) Biochim. Biophys. Acta 850, 333–342.

70 Zimmermann, J.L. and Rutherford, A.W. (1984) Biochim. Biophys. Acta 767, 160–167.
71 De Paula, J.C., Beck, W.F. and Brudvig, G.W. (1986) J. Am. Chem. Soc. 108, 4002–4009.
72 Thompson, L.K. and Brudvig, G.W. (1988) Biochemistry 27, 6653–6658.
73 Babcock, G.T., Widger, W.R., Cramer, W.A., Oertling, W.A. and Metz, J.G. (1985) Biochemistry 24, 3638–3645.
74 Crowder, M.S., Prince, R.C. and Bearden, A. (1982) FEBS Lett. 144, 204–208.
75 Thompson, L.K., Miller, A.-F., Buser, C.A., De Paula, J.C. and Brudvig, G.W. (1989) Biochemistry 28, 8048–8056.
76 Cramer, W.A. and Whitmarsh, J. (1977) Annu. Rev. Plant Physiol. 28, 133–172.
77 Larsson, C., Jansson, C., Ljungberg, U.L., Akerlund, H.E. and Andersson, B. (1984) in Advances in Photosynthesis Research (Sybesma, C., ed.), Vol. 1, pp. 363–366, Martinus Nijhoff/Dr. W. Junk, Dordrecht.
78 Malkin, R. and Vänngård, T. (1980) FEBS Lett. 111, 228–231.
79 Nugent, J.H.A. and Evans, M.C.W. (1980) FEBS Lett. 112, 1–4.
80 Malkin, R. and Bearden, A.J. (1973) Proc. Natl. Acad. Sci. USA 70, 294–297.
81 Visser, J.W.M. and Rijgersberg, C.P. (1974) in the Proceedings of the Third International Congress on Photosynthesis (Avron, M., ed.), pp. 399–408, Elsevier, Amsterdam.
82 Miller, A.-F. and Brudvig, G.W. (1990) Biochemistry 29, 1385–1392.
83 Miller, A.-F., De Paula, J.C. and Brudvig, G.W. (1987) Photosynth. Res. 12, 205–218.
84 Nugent, J.H.A., Telfer, A., Demetriou, C. and Barber, J. (1990) FEBS Lett. 255, 53–58.
85 Tiede, D.M., Prince, R.C., Reed, G.H. and Dutton, P.L. (1976) FEBS Lett. 65, 301–304.
86 Klimov, V.V., Dolan, E. and Ke, B. (1980) FEBS Lett. 112, 97–100.
87 Frank, H.A., Hansson, Ö. and Mathis, P. (1989) Photosynth. Res. 20, 279–289.
88 Prince, R.C., Tiede, D.M., Thornber, J.P. and Dutton, P.L. (1977) Biochim. Biophys. Acta 462, 467–490.
89 Babcock, G.T. and Sauer, K. (1975) Biochim. Biophys. Acta 376, 315–328.
90 Ono, T. and Inoue, Y. (1989) Biochim. Biophys. Acta 973, 443–449.
91 Metz, J.G., Nixon, P.J., Rögner, M., Brudvig, G.W. and Diner, B.A. (1989) Biochemistry 28, 6960–6969.
92 Debus, R.J., Barry, B.A., Sithole, I., Babcock, G.T. and McIntosh, L. (1988) Biochemistry 27, 9071–9074.
93 Hoganson, C.W. and Babcock, G.T. (1988) Biochemistry 27, 5848–5855.
94 Lozier, R.H. and Butler, W.L. (1974) Biochim. Biophys. Acta 333, 465–480.
95 Malkin, R. and Bearden, A.J. (1975) Biochim. Biophys. Acta 396, 250–259.
96 Ghanotakis, D.F. and Babcock, G.T. (1983) FEBS Lett. 153, 231–234.
97 Bock, C.H., Gerken, S., Stehlik, D. and Witt, H.T. (1988) FEBS Lett. 227, 141–146.
98 Hoganson, C.W. and Babcock, G.T. (1989) Biochemistry 28, 1448–1454.
99 Ghanotakis, D.F., De Paula, J.C., Demetriou, D.M., Bowlby, N.R., Petersen, J., Babcock, G.T. and Yocum, C.F. (1989) Biochim. Biophys. Acta 974, 44–53.
100 Davis, M.S., Forman, A. and Fajer, J. (1979) Proc. Natl. Acad. Sci. USA 76, 4170–4174.
101 Rutherford, A.W., Paterson, D.R. and Mullet, J.E. (1981) Biochim. Biophys. Acta 635, 205–214.
102 Dutton, P.L., Leigh, J.S. and Seibert, M. (1972) Biochem. Biophys. Res. Commun. 46, 406–413.
103 Thurnauer, M.C., Katz, J.J. and Norris, J.R. (1975) Proc. Natl. Acad. Sci. USA 72, 3270–3274.
104 Durrant, J.R., Giorgi, L.B., Barber, J., Klug, D.R. and Porter, G. (1990) Biochim. Biophys. Acta 1017, 167–175.
105 Rutherford, A.W. (1986) Biochem. Soc. Trans. 14, 15–17.
106 Van Mieghem, F.J.E., Nitschke, W., Mathis, P. and Rutherford, A.W. (1989) Biochim. Biophys. Acta 977, 207–214.
107 Okamura, M.Y., Satoh, K., Isaacson, R.A. and Feher, G. (1987) in Progress in Photosynthesis Research (Biggins, J., ed.), Vol. I, pp. 379–381, Martinus Nijhoff/Dr. Junk, Dordrecht.
108 Diner, B.A. and Petrouleas, V. (1987) Biochim. Biophys. Acta 895, 107–125.
109 Petrouleas, V. and Diner, B.A. (1987) Biochim. Biophys. Acta 893, 126–137.
110 Petrouleas, V. and Diner, B.A. (1986) Biochim. Biophys. Acta 849, 264–275.
111 Bowlby, N., Petersen, J., Babcock, G.T. and Yocum, C.F. (1989) Physiol. Plant. 76, A114.
112 Itoh, S., Tang, X.-S. and Satoh, K. (1986) FEBS Lett. 205, 275–281.
113 Aasa, R., Andréasson, L.-E., Styring, S. and Vänngård, T. (1989) FEBS Lett. 243, 156–160.
114 Petrouleas, V. and Diner, B.A. (1990) Biochim. Biophys. Acta 1015, 131–140.
115 Boussac, A., Zimmermann, J.L., Rutherford, A.W. and Lavergne, J. (1990) Nature 347, 303–306.
116 Sivaraja, M. and Dismukes, G.C. (1988) Biochemistry 27, 6297–6306.
117 Beck, W.F. and Brudvig, G.W. (1987) Biochemistry 26, 8285–8295.
118 Nitschke, W. and Hauska, G. (1987) Biochim. Biophys. Acta 892, 314–319.
119 Rich, P.R., Heathcote, P., Evans, M.C.W. and Bendall, D.S. (1980) FEBS Lett. 116, 51–56.
120 Bergström, J. and Vänngård, T. (1982) Biochim. Biophys. Acta 682, 452–456.
121 Malkin, R. and Bearden, A.J. (1978) Biochim. Biophys. Acta 505, 147–181.
122 Prince, R.C., Crowder, M.S. and Bearden, A.J. (1980) Biochim. Biophys. Acta 592, 323–337.
123 Malkin, R. and Aparicio, P.J. (1975) Biochem. Biophys. Res. Commun. 63, 1157–1160.
124 Rutherford, A.W. and Heathcote, P. (1985) Photosyn. Res. 6, 295–316.
125 Commoner, B., Townsend, J. and Pake, G.E. (1954) Nature 174, 689–691.
126 Beinert, H., Kok, B. and Hoch, G. (1962) Biochem. Biophys. Res. Commun. 7, 209–212.
127 Frank, H.A., McLean, M.,B. and Sauer, K. (1979) Proc. Natl. Acad. Sci. USA 76, 5124–5128.
128 Rutherford, A.W. and Mullet, J.E. (1981) Biochim. Biophys. Acta 635, 225–235.
129 Biggins, J., Tanguay, N.A. and Frank, H.A. (1989) FEBS Lett. 250, 271–274.
130 Iwaki, M. and Itoh, S. (1989) FEBS Lett. 256, 11–16.
131 Barry, B.A., Bender, C.J., McIntosh, L., Ferguson-Miller, S. and Babcock, G.T. (1989) Isr. J. Chem. 28, 129–132.
132 Ziegler, K., Lockau, W. and Nitschke, W. (1987) FEBS Lett. 217, 16–20.
133 Petrouleas, V., Brand, J.J., Parrett, K.G. and Golbeck, J.H. (1989) Biochemistry 28, 8980–8983.
134 Noodleman, L., Norman, J.G., Jr., Osborne, J.H., Aizman, A. and Case, D.A. (1985) J. Am. Chem. Soc. 107, 3418–3426.
135 Dismukes, G.C. and Sauer, K. (1978) Biochim. Biophys. Acta 504, 431–445.
136 Aasa, R., Bergstrom, J. and Vänngård, T. (1981) Biochim. Biophys. Acta 637, 118–123.
137 Aasa, R. (1970) J. Chem. Phys. 52, 3919–3930.

138 Sibbald, P.R. and Green, B.R. (1987) Photosyn. Res. 14, 201–209.
139 Blumberg, W.E. and Peisach, J. (1966) Biochim. Biophys. Acta 126, 269–273.
140 Visser, J.W.M., Amesz, J. and Van Gelder, B.F. (1974) Biochim. Biophys. Acta 333, 279–287.
141 Peisach, J. and Blumberg, W.E. (1974) Arch. Biochem. Biophys. 165, 691–708.
142 Reed, G.H. and Markham, G.D. (1984) in Biological Magnetic Resonance (Berliner, L.J. and Reuben, J., eds.), Vol. 6, pp. 73–142, Plenum Press, New York.
143 Yocum, C.F., Yerkes, C.T., Blankenship, R.E., Sharp, R.R. and Babcock, G.T. (1981) Proc. Natl. Acad. Sci. USA 78, 7507.
144 Tinkham, M. and Strandberg, M.W.P. (1955) Phys. Rev. 97, 937–951.
145 Tinkham, M. and Strandberg, M.W.P. (1955) Phys. Rev. 97, 951–966.
146 Beringer, R. and Castle, J.G., Jr. (1951) Phys. Rev. 81, 82–88.
147 De Paula, J.C. (1987) Ph. D. Thesis, Yale University, New Haven, CT.
148 Miller, A.-F. and Brudvig, G.W. (1989) Biochemistry 28, 8181–8190.
149 Tamura, N. and Cheniae, G.M. (1987) Biochim. Biophys. Acta 890, 179–194.
150 Aasa, R., Andréasson, L.-E., Lagenfelt, G. and Vänngård, T. (1987) FEBS Lett. 221, 245–248.